JOURNAL OF SOLID STATE CHEMISTRY 72, 330–337 1988)

The Nonstoichiometric Defect Structure and Transport Properties of CeO_{2-x} in the Near-stoichiometric Composition Range

EDWARD K. CHANG AND R. N. BLUMENTHAL

Department of Materials Science and Metallurgy, Marquette University, Milwaukee, Wisconsin 53233

Received October 31, 1986; in revised form June 15, 1987

The electrical conductivity of undoped polycrystalline CeO_{2-x} was measured in the temperature range 800–1000°C and $1–10^{-3}$ atm of oxygen partial pressures. It was found that the results were consistent with a defect model involving doubly ionized oxygen vacancies arising from both impurities and nonstoichiometry. Based on this model the conductivity results were analyzed to determine the effective concentration of the lower valent impurities. The ionic transference number obtained from the analysis agrees with that measured using the electrochemical cell technique. It was also found that the effect of the lower valent impurities can be compensated by counterdoping with Ta_2O_5. The fully compensated specimen exhibits the predicted behavior of pure ceria (i.e., $\sigma \alpha P_{O_2}^{-1/6}$). The relative oxygen partial molal enthalpy, $\Delta\bar{H}_{O_2}$, of ceria was calculated from the temperature dependence of the conductivity of the counterdoped specimen at constant P_{O_2}. The value of $\Delta\bar{H}_{O_2}$ thus obtained, 9.96 ± 0.66 eV, is in good agreement with previously reported values obtained from thermogravimetric measurements.

I. Introduction

Nonstoichiometric cerium dioxide, ceria (i.e., CeO_{2-x}), has been the subject of many investigations (*1–13*). Based on the results of these studies, ceria may be classified as an oxygen deficient *n*-type semiconductor. The electronic conduction takes place via a hopping-type mechanism (*8, 9*). The extensive single-phase region of CeO_{2-x} at elevated temperatures permits the deviation from stoichiometry, x, and the electrical conductivity, σ, to be studied over a wide range of partial pressures of oxygen, P_{O_2} (*5–13*).

Although there is general agreement that the predominant type of point defect is the oxygen vacancy, there are different interpretations concerning the state of ionization of the oxygen vacancies in the regions of P_{O_2} and temperature where the $-\frac{1}{5}$ dependence of x and σ on P_{O_2} is observed (*5–11*). Recently, it was found that the disagreement with respect to ionization state was the result of neglecting the effect of lower valent cation impurities in ceria (*12*).

The major impurities in ceria were found to be those of lower valent cations (i.e., Ca^{+2}) (*14*). The substitutional incorporation of CaO in CeO_{2-x} produces charge compensating doubly ionized oxygen vacancies (*15–17*). Consequently, these impurities would influence the P_{O_2} dependence of the measured properties, especially in the near-stoichiometric composition range (i.e., small values of x). Dawicke and Blumenthal (*12*), taking CaO impurities into account, have shown that the experimentally ob-

0022-4596/88 $3.00

served $P_{O_2}^{-1/5}$ dependence of both σ and x is consistent with a defect model involving only doubly ionized oxygen vacancies. The relation, $x\alpha P_{O_2}^{-1/6}$, only holds true in pure CeO_{2-x}. For ceria containing lower valent impurities, the relation should be $x\alpha P_{O_2}^{-1/4}$ in the near-stoichiometric composition range. However, due to difficulties in obtaining small values of x, experimental data in support of $P_{O_2}^{-1/4}$ has not been obtained. Therefore, it is important to study the effect of impurities and to determine the types and the equivalent amounts of these impurities and, optimally, to compensate for their effects such that the predicted P_{O_2} dependence of pure CeO_2 can be obtained.

II. Theory

Ceria samples used by all investigators contain lower valent cation impurities. For example, samples used in this laboratory usually have the designated purities of 99.9% (3 *N* CeO_{2-x}), 99.99% (4 *N* CeO_{2-x}), and 99.999% (5 *N* CeO_{2-x}); all designations are with respect to the total rare earth oxides. These materials reportedly contain a calcium impurity of 200 to 300 ppm by weight, and may be considered to have been doped with 0.1 mole% calcia (*14*). Calcium is known to substitute for cerium producing charge compensating doubly ionized oxygen vacancies (*15–17*), which is also the nonstoichiometric defect. Dawicke and Blumenthal (*12*) examined the P_{O_2} dependence of x as a function of CaO dopant concentration. They found that CaO impurities have a significant effect in the region where x is small. Although they assumed CaO to be the only impurity, similar results would apply for any M^{+2} or M^{+3} dopant producing charge compensating oxygen vacancies. Therefore, the impurity considered in this study is CaO, in accord with Dawicke and Blumenthal, and the amount of calcia is the equivalent of the sum of all lower valent impurities.

The overall nonstoichiometric reaction to be considered is

$$Ce_{1-y}Ca_yO_{2-y} = Ce_{1-y}Ca_yO_{2-y-x} + \frac{x}{2}O_2(g). \quad (1)$$

while in the Kroger–Vink notation (*18*), the defect reaction is

$$2Ce_{Ce}^{x} + O_O^x = 2Ce_{Ce}' + V_O^{\cdot\cdot} + \tfrac{1}{2}O_2(g). \quad (2)$$

In the above reaction, the electrons are explicitly written as occupying cerium sites because conduction in ceria is known to proceed via a hopping-type mechanism. The mass action constant associated with reaction (2) is

$$K_{ma} = \frac{[Ce_{Ce}']^2[V_O^{\cdot\cdot}]P_{O_2}^{1/2}}{[O_O^x][Ce_{Ce}^x]^2}, \quad (3)$$

where the bracketed terms are site fractions for each corresponding species. Applying site conversion and the electroneutrality condition (*7*), the mass action constant may be written as

$$K_{ma} = \frac{(2x)^2\left(\frac{x+y}{2}\right)}{(1-y-2x)^2\left(1-\frac{y}{2}-\frac{x}{2}\right)} \times P_{O_2}^{-1/2}. \quad (4)$$

The P_{O_2} dependence of x, as a function of x and y, has been discussed by Dawicke and Blumenthal (*12*). They pointed out that, with a defect model involving $V_O^{\cdot\cdot}$ only, the P_{O_2} dependence of x should approach a value of $-\frac{1}{4}$ in the region where $x < 10^{-4}$, with a nominal y value of 0.1 mole%. However, this dependence has not been experimentally obtained because of the limitations in measuring small values of x (*7, 12*).

Since the electronic conductivity, σ_e, is proportional to x, the P_{O_2} dependence of the total conductivity, σ_t, can be derived based on the law of mass action. While small values of x are difficult to measure, σ_t can be accurately determined in the high P_{O_2} re-

gion. This enables the defect model to be tested in the near-stoichiometric composition range. The two major charge carrier species involved in ceria are $V_{\ddot{O}}$ and Ce'_{Ce}. The total electrical conductivity can be expressed as

$$\sigma_t = \frac{8x}{a_0^3} \times e \times \mu_e + \frac{8(x+y)}{a_0^3} \times e \times \mu_{V_{\ddot{O}}}, \quad (5)$$

where a_0 is the lattice parameter.

In the low temperature and high P_{O_2} region where x is small and $y \gg x$, ceria shows mixed conduction, ionic and electronic, even though $\mu_{V_{\ddot{O}}}$ is considerably smaller than μ_e (*19, 20*). For this limiting case (i.e., $1 \gg y \gg x$), the denominator of the mass action expression in Eq. (4) may be neglected, and, since $x \ll y$ in this region, Eq. (4) can be simplified to

$$K_{ma} = 2x^2 \times y \times P_{O_2}^{1/2}. \quad (6)$$

If Eq. (6) is used to solve x, then

$$x = \sqrt{\frac{K_{ma}}{2y}} \times P_{O_2}^{-1/4}. \quad (7)$$

Eq. (5) can thus be rewritten as

$$\mu_t = \frac{8}{a_0^3} \times e \times \mu_e \times \sqrt{\frac{K_{ma}}{2y}} \times P_{O_2}^{-1/4} + \frac{8y}{a_0^3} \times e \times \mu_{V_{\ddot{O}}}. \quad (8)$$

The second term on the right hand side of Eq. (8) is independent of P_{O_2}. Therefore, Eq. (8) can be tested by plotting σ_t vs $P_{O_2}^{-1/4}$ in the near-stoichiometric range. A linear relationship would confirm this limiting case treatment.

If the above analysis is correct, the slope of the straight line can be related to the mass action constant as

$$\text{slope} = \frac{8}{a_0^3} \times e \times \mu_e \times \sqrt{\frac{K_{ma}}{2y}}. \quad (9)$$

Since all parameters except y in Eq. (9) are known (*4, 12*), the "calcia" content, y, can be calculated.

The intercept of the straight line is the partial conductivity due to the charge compensating $V_{\ddot{O}}$, and denoted by $\sigma_{V_{\ddot{O}}}$, and

$$\sigma_{V_{\ddot{O}}} = \frac{8y}{a_0^3} \times e \times \mu_{V_{\ddot{O}}}. \quad (10)$$

$\sigma_{V_{\ddot{O}}}$ should be a good approximation of the ionic conductivity of ceria in the near-stoichiometric composition range because the change in $[V_{\ddot{O}}]$ due to nonstoichiometry is relatively small (i.e., $y \gg x$). Therefore, the ionic transference number may be obtained by

$$t_i(T, P_{O_2}) = \frac{\sigma_{V_{\ddot{O}}}(T)}{\sigma_t(T, P_{O_2})}. \quad (11)$$

Another limiting case of interest is for the region where $x \gg y$. However, defect interactions in ceria become significant at $\log x > -2.4$ (*7, 12, 14*), and since the impurity content, y, is inherently large, the law of mass action is not applicable for $x \gg y$. Thus, to obtain the predicted $P_{O_2}^{-1/6}$ dependence of σ and x, the value of y would have to be reduced. This may be accomplished through counterdoping. When ceria is doped with Ta_2O_5, a donor, the charge compensating defect is Ce'_{Ce} (*21*). On the other hand, the lower valent impurities (e.g., Ca^{2+}), substituting for cerium, are essentially acceptors. When donors and acceptors are present simultaneously, compensation results and the concentration of the remaining defect (i.e., $[Ce'_{Ce}]$ or $[V_{\ddot{O}}]$) is determined by the net excess of their concentrations.

The electroneutrality condition of the counterdoped system (ceria doped with Ta_2O_5 to compensate for "CaO" impurities) is

$$[Ce'_{Ce}] + 2[Ca''_{Ce}] = [Ta'_{Ce}] + 4[V_{\ddot{O}}]. \quad (12)$$

Thus, if ceria is appropriately doped with Ta_2O_5 the effect of the lower valent impurities can be fully compensated, and Eq. (12) can be simplified to

$$[Ce'_{Ce}] = 4[V''_{O}]. \quad (13)$$

Eq. (13) is identical to the electroneutrality condition of pure ceria (*7*). Therefore, properly counterdoped ceria should behave as pure ceria (i.e., $Ce_{1-3y}Ca_yTa_{2y}O_{2-x}$). In this case, Eq. (4) can be written as

$$K_{ma} = 2x^3 \times P_{O_2}^{1/2}. \quad (14)$$

Since $\mu_e > \mu_{V''_O}$ (*19, 20*), the conductivity of counterdoped ceria is predominantly electronic, and it is apparent from Eqs. (5) and (14) that

$$\sigma_t \alpha x \alpha K_{ma}^{1/3} \times P_{O_2}^{-1/6}. \quad (15)$$

Experimental conductivity data exhibiting an isothermal $P_{O_2}^{-1/6}$ dependence would indicate that the impurities in the sample are fully compensated. Thus, the electrical conductivity of the appropriately counterdoped sample is truly representative of the charge carriers arising from nonstoichiometry. For this case, the standard enthalpy change, $\Delta H°$, associated with Eq. (2), can be obtained from the temperature dependence of the conductivity at constant P_{O_2}. Since

$$\mu_e = \mu_e^0 \exp(-Q/kT), \quad (16)$$

where Q is the activation energy for electron motion (*8, 12, 22*), it can be seen from Eqs. (5), (15), and (16) that (*23*)

$$\sigma_t \alpha P_{O_2}^{-1/6} \times \exp\left[-\left(\frac{\Delta H°}{3} + Q\right)/k \times T\right], \quad (17)$$

it follows that at a constant temperature, σ_t is proportional to $P_{O_2}^{-1/6}$. Eq. (17) also suggests that at a constant oxygen pressure, a plot of log σ_t vs $1/T$ would yield a straight line with a slope of $-(\Delta H°/3 + Q)/2.303 \times k$. Since Q is known (*8, 12, 22*), the quantity $\Delta H°$ can be obtained. For ceria, as a consequence of the dilute solution behavior for a defect mechanism of doubly ionized oxygen vacancies and electrons localized on cerium sites, the relative oxygen partial molal enthalpy is (*7*)

$$\Delta \bar{H}_{O_2} = -2\Delta H°. \quad (18)$$

Thus, the thermodynamic quantity, $\Delta \bar{H}_{O_2}$, can be determined from the conductivity measurement for the fully compensated condition.

III. Experimental

In this study, sintered specimens of ceria and ceria doped with Ta_2O_5 were used for all measurements. The samples were prepared from CeO_2 powder having a designated purity of 99.9% (3 *N* CeO_2). This purity designation is with respect to rare earth impurities only. Table I shows the chemical analysis of this material (obtained from the product data accompanying the material). The tantalum pentoxide was purchased from Matheson, Coleman and Bell. Doped specimens were prepared by intimate mixing of appropriate proportions of the metal oxide powders. They were pressed into bars of dimensions $2 \times \frac{1}{4} \times \frac{1}{4}$ in. and pellets of $\frac{3}{4}$ in. diameter. A surface layer was scraped off to avoid contamination from the die walls. They were placed in alumina boats and covered with powders of the same composition to minimize the change in sample composition during the sintering

TABLE I

CHEMICAL ANALYSIS OF CeO_2 POWDER[a]

CeO_2/REO[b]	99.9%
La_2O_3/REO	40 ppm
Nd_2O_3/REO	20 ppm
Pr_6O_{11}/REO	20 ppm
CaO	300 ppm
SrO	50 ppm
Fe_2O_3	50 ppm
MnO_2	20 ppm
Na_2O	2000 ppm

[a] Obtained from the product data of Molycorp.

[b] Total rare earth oxides.

process. A glowbar furnace was used to sinter the samples at 1470°C in air for 10 hr.

The pellets were used to measure the transference number, while the bars were used for the conductivity measurements. The bulk density of specimens was determined from the mass and the volume, which was obtained from the external dimensions of the specimen. In this study, the density of all sintered specimens is in excess of 80% of the theoretical density.

The standard four-probe d.c. technique was employed for the electrical conductivity measurements. The apparatus was the same as that described in a previous publication (*6*). Equilibrium was assumed when the potential across the inner probe remained unchanged. The measured values of the conductivity, $\sigma_{\text{meas.}}$, were normalized for porosity (*24*).

The ionic transference number was measured by an electrochemical cell technique. The apparatus was the same as that described elsewhere (*19*). Pure oxygen and 10% O_2–Ar were used to maintain the oxygen potentials at the two electrodes. The average ionic transference number was obtained from

$$\bar{t}_i = E_{\text{meas.}}/E_{\text{th}}, \qquad (19)$$

where $E_{\text{meas.}}$ is the emf measured and E_{th} is the theoretical emf.

IV. Results and Discussion

The electrical conductivity of undoped 3 *N* CeO_{2-x} was measured as a function of P_{O_2} between 1 and 10^{-19} atm in the temperature range 800 to 1000°C. Figure 1 shows the isothermal plots of log σ_t vs log P_{O_2} at 100°C intervals. For comparative purposes, the conductivity of undoped 5 *N* CeO_{2-x} measured by Blumenthal *et al.* (*6*) is shown as solid lines in the figure. A qualitative description of the data may be given in terms of two regions as follows:

Region 1. In the low temperature and high P_{O_2} region (i.e., small values of x), the impurities significantly influence the magnitude and the P_{O_2} dependence of the conductivity. For example, σ of 5 *N* CeO_{2-x}, a purer material, exhibits approximately a $-\frac{1}{5}$ dependence on P_{O_2} whereas 3 *N* CeO_{2-x} has a higher conductivity which is less dependent on P_{O_2}.

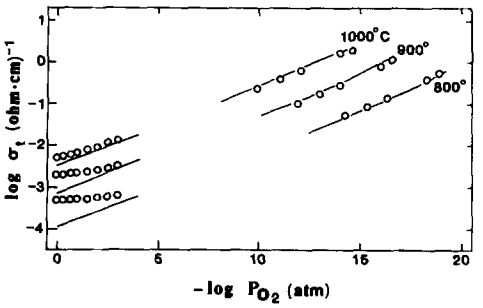

FIG. 1. Isothermal plots of log σ_t vs log P_{O_2} for undoped CeO_{2-x} of different purities. ○, 3 *N* CeO_{2-x}; —, 5 *N* CeO_{2-x} (*10*).

Region 2. At higher temperatures, and particularly in the low P_{O_2} region (i.e., larger values of x), the conductivities of these two samples are essentially the same. The impurities are less effective in this region, because σ_t is controlled by the nonstoichiometric defects.

Since one of the objectives of this study is to investigate the impurity effects, emphasis was placed on the results in Region 1 for 3 *N* CeO_{2-x}. In this near-stoichiometric composition range, a nonlinear relationship exists between log σ_t and log P_{O_2} and the conductivity is less dependent on P_{O_2} at lower temperatures. These observations are consistent with a model involving lower valent cation impurities. From Eq. (8), σ_t should be proportional to P_{O_2} to the $-\frac{1}{4}$ power. Figure 2 shows the linear plots of σ_t vs $P_{O_2}^{-1/4}$ at 1000 and 900°C. For the 800°C isotherm, a similar plot was not presented because the dependence of σ_t on P_{O_2} is not significant.

The slopes shown in Fig. 2 are temperature dependent only. They can be related to

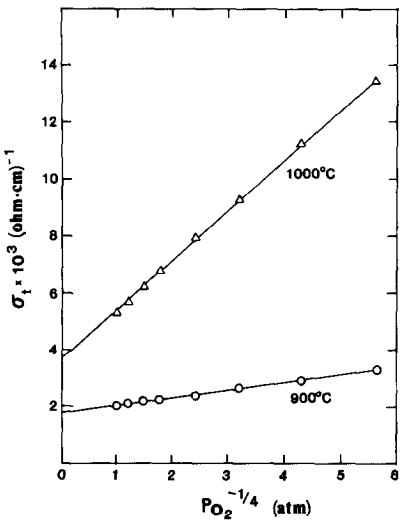

FIG. 2. Isothermal plots of σ_t vs $P_{O_2}^{-1/4}$ for undoped 3 N CeO_{2-x}.

the "calcia" content, y, according to Eq. (9). From the 1000°C isotherm, the calculated value of the slope was 1.8×10^{-3}. If the values 1.1×10^{-12} for K_{ma} (*12*), 5.47 Å for a_o (*4*), and 0.012 ($cm^2/V \times s$) for μ_e (*12*) were used, y was calculated to be $\simeq 0.0015$. From the 900°C isotherm, the calculated value of the slope was 2.4×10^{-4}. Similarly, if 2.4×10^{-14} for K_{ma}, 5.46 Å for a_o, and 0.01 for μ_e were used, y was calculated to be $\simeq 0.0013$.

The calculation of y involves the parameters (i.e., K_{ma}, a_o, and μ_e) experimentally determined from independent investigations. The small difference between the values of y calculated at 900 and 1000°C is most likely the result of the errors in choosing these parameters plus the experimental error involved in this study. However, a calcia impurity content of 450 ppm by weight is equivalent to a value of $y = 0.0014$. When compared with the chemical analysis shown in Table 1, the calculated value of y appears to be reasonable.

By knowing the value of y, the intercepts of the straight lines shown in Fig. 2 can be used to calculate the mobility of the oxygen vacancies according to Eq. (10). The calculated values of $\mu_{V_O^{\cdot\cdot}}$ were 3.1×10^{-4} ($cm^2/V \times s$) at 1000°C and 1.8×10^{-4} ($cm^2/V \times s$) at 900°C. These values are within 20% of those obtained by Reddy (*20*).

These intercepts can also be used to obtain the ionic transference number according to Eq. (11). By this method, the calculated values of t_i were 0.69 and 0.52 at 1000°C and 0.87 and 0.78 at 900°C for P_{O_2} of 1 and 0.1 atm, respectively.

To check these calculations, the average ionic transference number of 3 N CeO_{2-x} between P_{O_2} of 1 and 0.1 atm was measured using an electrochemical cell technique in the temperature range 800–1000°C. The results are shown in Fig. 3. It can be seen that the values of t_i measured are in good agreement with those calculated from the conductivities.

By employing the same technique, Van Handel and Blumenthal (*19*) reported that t_i was $\simeq 0.2$ at 1000°C and $\simeq 0.6$ at 900°C in a similar P_{O_2} region. The difference in the results is most likely a consequence of using starting materials with different impurity levels.

The results of this study are consistent

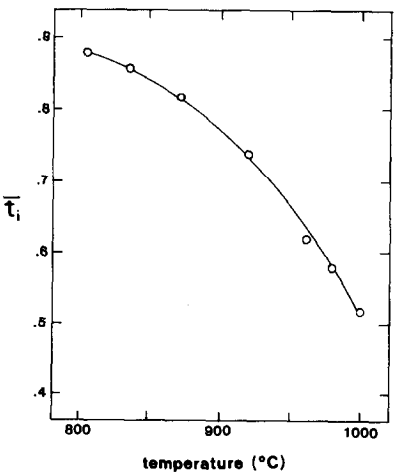

FIG. 3. Plot of $\bar{t}_i$ vs temperature in the P_{O_2} range 0.1 to 1.0 atm for undoped 3 N CeO_{2-x}.

with a point defect model only involving doubly ionized oxygen vacancies when lower valent cation impurities are taken into consideration. The impurity effect may be fully compensated by the counterdoping experiment, as described under Theory. The sample then should behave as pure ceria and the predicted $P_{O_2}^{-1/6}$ dependence of σ_t should be obtained.

Ceria with lower valent cation impurities was treated in this study as $Ce_{1-y}Ca_yO_{2-y-x}$. Ceria doped with Ta_2O_5 has the formula $Ce_{1-z}Ta_zO_{2+z/2-x}$ when impurities are not included. However, if Ta_2O_5 and CaO are simultaneously present, the system may be expressed as $Ce_{1-y-z}Ca_yTa_zO_{2-y+z/2-x}$. When the amount of Ta_2O_5 added to ceria is equivalent to the "CaO" impurity content (i.e., $y = z/2$), the fully counterdoped system behaves as pure ceria.

The results of the conductivity measurement for a specimen of 0.1 mole% Ta_2O_5 doped 3 N CeO_{2-x} are shown in Fig. 4 as isothermal plots of log σ_t vs log P_{O_2}. For comparative purposes, data obtained with the undoped 3 N CeO_{2-x} are also included as dashed lines. It is observed that the fully

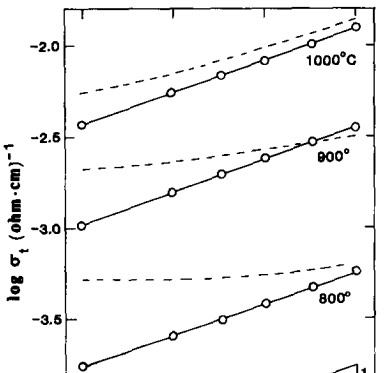

FIG. 4. Isothermal plots of log σ_t vs log P_{O_2}. ---, undoped 3 N CeO_{2-x}; —○—, 0.1 mole% Ta_2O_5 doped 3 N CeO_{2-x}.

counterdoped sample exhibits a more pronounced P_{O_2} dependence of σ_t than the undoped 3 N CeO_{2-x}. Furthermore, the slopes of log σ_t vs log P_{O_2} for the counterdoped sample are close to $-\frac{1}{6}$ for the three isotherms. This result is consistent with the doubly ionized oxygen vacancy defect model for pure ceria.

To obtain a $-\frac{1}{6}$ dependence in the region studied, the amount of Ta_2O_5 doping may have to be controlled to a few parts per million of the "CaO" impurity content. The amount of "CaO" calculated from conductivity data was approximately 0.14 mole%. The difference between 0.14 and 0.1 mole has to be errors in preparing samples with a small dopant concentration. The P_{O_2} dependence of σ_t provides a sensitive indication of the effective dopant level. It appears fortuitous that the "CaO" impurities were fully compensated with ~0.1 mole% Ta_2O_5 counterdoping.

As discussed in the theory, the standard enthalpy change associated with the nonstoichiometric defect reaction may be obtained from the temperature dependence of σ_t for the counterdoped specimen. Using the least-squares technique, an experimental activation energy of 1.87 ± 0.11 eV was calculated from the slope of the line in Fig. 5 where log σ_t is plotted vs $10^3/T$. By equating the experimental activation energy with Eq. (17),

$$\frac{\Delta H^\circ}{3} + Q = 1.87 \pm 0.11 \text{ (eV)}. \quad (20)$$

By using 0.21 eV as the activation energy for electron motion (*12, 22*), the calculated value of ΔH° was 4.98 ± 0.33 eV. Thus, $\Delta \bar{H}_{O_2}$, the relative oxygen partial molal enthalpy of ceria, is −9.96 ± 0.66 eV (from Eq. (18)). This result is in good agreement with the value (i.e., ~10 eV) obtained at larger departures from stoichiometry (i.e., $x \simeq 10^{-3}$) using thermogravimetric measurement (*7, 12*).

It should be noted that the thermogravi-

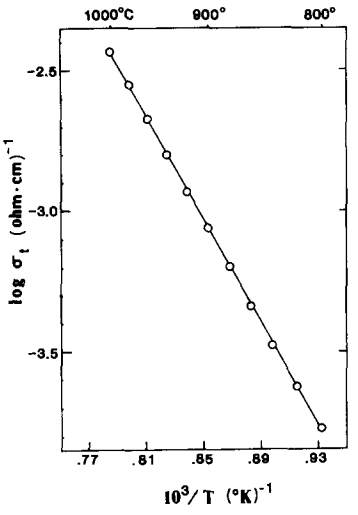

FIG. 5. Log σ_t vs $1/T$ for 0.1 mole% Ta_2O_5 doped 3 N CeO_{2-x} in pure oxygen.

metrically obtained $\Delta\bar{H}_{O_2}$ is the result of a direct measurement where no assumption was made. In this study, measurements and analysis on CeO_{2-x} were conducted in the near-stoichiometric composition range where the range of x is small. The calculation of $\Delta\bar{H}_{O_2}$ was based on the assumptions that oxygen vacancies are doubly ionized and the law of mass action is applicable in a dilute system. The agreement in $\Delta\bar{H}_{O_2}$ along with the $P_{O_2}^{-1/6}$ dependence of σ_t should justify both assumptions.

References

1. D. J. M. BEVAN AND J. KORDIS, *J. Inorg. Nucl. Chem.* **26,** 1509 (1964).
2. G. BRAUER AND K. A. GINGERICH, *J. Inorg. Nucl. Chem.* **16,** 87 (1960).
3. B. C. H. STEELE AND J. M. FLOYD, *Proc. Brit. Ceram. Soc.* **19,** 55 (1971).
4. J. R. SIMS AND R. N. BLUMENTHAL, *High Temp. Sci.* **8,** 99 (1976).
5. E. M. GREENER, J. M. WIMMER, AND W. M. HIRTHE, *Proc. Conf. Rare Earth Res. 4th,* p. 538, Phoenix, AZ (1964).
6. R. N. BLUMENTHAL, P. W. LEE, AND R. J. PANLENER, *J. Electrochem. Soc.* **118,** 123 (1971).
7. R. J. PANLENER, R. N. BLUMENTHAL, AND J. E. GARNIER, *J. Phys. Chem. Solids* **36,** 1213 (1975).
8. R. N. BLUMENTHAL AND R. L. HOFMAIER, *J. Electrochem. Soc.* **121,** 126 (1974).
9. H. L. TULLER AND A. S. NOWICK, *J. Phys. Chem. Solids* **38,** 859 (1977).
10. H. L. TULLER AND A. S. NOWICK, *J. Electrochem. Soc.* **126,** 209 (1979).
11. I. K. NAIK AND T. Y. TIEN, *J. Phys. Chem. Solids* **39,** 311 (1978).
12. J. W. DAWICKE AND R. N. BLUMENTHAL, *J. Electrochem. Soc.* **133,** 904 (1986).
13. E. H. BAKER, M. IQBAL, AND B. E. KNOX, *J. Mater. Sci.* **12,** 305 (1977).
14. R. J. PANLENER, Ph.D. Dissertation, Marquette University, Milwaukee, WI (1972).
15. R. N. BLUMENTHAL, F. S. BRUGNER, AND J. E. GARNIER, *J. Electrochem. Soc.* **120,** 1230 (1973).
16. H. L. TULLER AND A. S. NORWICK, *J. Electrochem. Soc.* **122,** 255 (1975).
17. J. E. GARNIER, R. N. BLUMENTHAL, R. J. PANLENER, AND R. K. SHARMA, *J. Phys. Chem. Solids* **37,** 369 (1976).
18. F. A. KROGER AND H. J. VINK, *Solid State Phys.* **3,** 310 (1956).
19. G. J. VAN HANDEL AND R. N. BLUMENTHAL, *J. Electrochem. Soc.* **121,** 1198 (1974).
20. S. N. S. REDDY, Ph.D. Dissertation, Marquette University, Milwaukee, WI (1977).
21. R. K. SHARMA, Ph.D. Dissertation, Marquette University, Milwaukee, WI (1977).
22. M. J. MASON, M.S. Thesis, Marquette University, Milwaukee, WI (1978).
23. E. K. CHANG, Ph.D. Dissertation, Marquette University, Milwaukee, WI (1984).
24. F. S. BRUGNER AND R. N. BLUMENTHAL, *J. Amer. Ceram. Soc.* **54,** 57 (1971).